Neuroscience 280 (2014) 275–281

IMPAIRED SYNAPTIC VESICLE RECYCLING CONTRIBUTES TO PRESYNAPTIC DYSFUNCTION IN LIPOPROTEIN LIPASE-DEFICIENT MICE

X. LIU,[a] B. ZHANG,[b] H. YANG,[a] H. WANG,[a] Y. LIU,[a] A. HUANG,[c] T. LIU,[a] X. TIAN,[a] Y. TONG,[a] T. ZHOU,[a] T. ZHANG,[a] G. XING,[a] W. XIAO,[d] X. GUO,[d*] D. FAN,[d*] X. HAN,[e] G. LIU,[f*] Z. ZHOU[b*] AND D. CHUI[a,c*]

[a] *Neuroscience Research Institute & Department of Neurobiology, Key Laboratory for Neuroscience of Ministry of Education and Ministry of Public Health, Health Science Center, Peking University, Beijing 100191, China*

[b] *Institute of Molecular Medicine, Peking University, Beijing 100871, China*

[c] *School of Medicine, University of Wisconsin-Madison, Madison, WI 53706, USA*

[d] *Peking University Third Hospital, Beijing 100191, China*

[e] *Diabetes and Obesity Research Center, Sanford/Burnham Medical Research Institute, La Jolla, CA 92037, USA*

[f] *Institute of Cardiovascular Science, Health Science Center, Peking University, Beijing 100191, China*

Abstract—Lipoprotein lipase (LPL) is expressed at high levels in hippocampal neurons, although its function is unclear. We previously reported that LPL-deficient mice have learning and memory impairment and fewer synaptic vesicles in hippocampal neurons, but properties of synaptic activity in LPL-deficient neurons remain unexplored. In this study, we found reduced frequency of miniature excitatory postsynaptic currents (mEPSCs) and readily releasable pool (RRP) size in LPL-deficient neurons, which led to presynaptic dysfunction and plasticity impairment without altering postsynaptic activity. We demonstrated that synaptic vesicle recycling, which is known to play an important role in maintaining the RRP size in active synapses, is impaired in LPL-deficient neurons. Moreover, lipid assay revealed deficient docosahexaenoic acid (DHA) and arachidonic acid (AA) in the hippocampus of LPL-deficient mice; exogenous DHA or AA supplement partially restored synaptic vesicle recycling capability. These results suggest that impaired synaptic vesicle recycling results from deficient DHA and AA and contributes to the presynaptic dysfunction and plasticity impairment in LPL-deficient neurons.

Key words: lipoprotein lipase, presynaptic dysfunction, synaptic vesicle recycling, readily releasable pool (RRP), synaptic plasticity.

INTRODUCTION

Lipoprotein lipase (LPL) hydrolyzes the triacylglycerol (TG) components of circulating chylomicrons (CM) and very low-density lipoproteins (VLDL), thereby providing non-esterified fatty acids and 2-monoacylglycerol for tissue utilization (Mead et al., 2002; Merkel et al., 2002; Lafourcade et al., 2007). Expression of LPL has been identified in many tissues, including the brain of several mammalian species (Goldberg et al., 1989; Yacoub et al., 1990). Relatively high expression of LPL was found in the hippocampus (Ben-Zeev et al., 1990; Vilaro et al., 1990), which plays a critical role in learning and memory. Hyperchylomicronemia, caused by mutant LPL gene, may develop hippocampal dysfunction or even dementia symptoms (Heilman and Fisher, 1974; Chait et al., 1981). Moreover, LPL mutations are also associated with risk of Alzheimer's disease (Baum et al., 1999). A study conducted by our lab found learning and memory impairment as well as fewer presynaptic vesicles in LPL-deficient mice (Xian et al., 2009), which is consistent with earlier reports that LPL is localized in soma and presynaptic vesicles but not in postsynaptic density (Klinger et al., 2011).

Many types of lipids and lipid-related enzymes are involved in regulation of synaptic function (Rohrbough and Broadie, 2005). For example, omega-3 polyunsaturated fatty acids (PUFAs) regulate synaptic endocytosis and synaptic vesicle recycling (Marza et al., 2008; Ben Gedalya et al., 2009). Wang et al. found decreased omega-3 PUFAs in the brain of LPL-deficient mice (Wang et al., 2011). However, the role of LPL in synaptic function and its underlying mechanisms are unexplored.

In this study, we tested synaptic function at different levels in LPL-deficient neurons and found that impaired synaptic vesicle recycling, which results from a deficiency of docosahexaenoic acid (DHA) and arachidonic acid (AA), contributes to the presynaptic

*Corresponding authors. Address: 38 Xue yuan Road, Haidian District, Neuroscience Research Institute, Health Science Center, Peking University, Beijing 100191, China (D. Chui).
E-mail address: dchui@bjmu.edu.cn (D. Chui).

Abbreviations: AA, arachidonic acid; AP, action potential; CM, chylomicrons; CME, clathrin-mediated endocytosis; DHA, docosahexaenoic acid; DMSO, dimethyl sulfoxide; EGTA, ethylene glycol tetraacetic acid; EPSC, excitatory postsynaptic current; FAME, fatty acid methyl ester; fEPSPs, field excitatory postsynaptic potentials; GAPDH, glyceraldehyde-3-phosphate-dehydrogenase; HEPES, 4-(2-hydroxyethyl)-1-piperazineethanesulfonic acid; ISI, inter-stimuli intervals; LPL, lipoprotein lipase; mEPSCs, miniature excitatory postsynaptic currents; NMDA, N-methyl-D-aspartic acid; PBS, Phosphate-buffered saline; PPF, Paired-pulse facilitation; PSD-95, postsynaptic density protein 95; PTP, post-tetanic potentiation; PUFAs, polyunsaturated fatty acids; RRP, readily releasable pool; TG, triacylglycerol; TTX, tetrodotoxin; VLDL, very low-density lipoproteins; WT, wild type.

http://dx.doi.org/10.1016/j.neuroscience.2014.07.080
0306-4522/

dysfunction and plasticity impairment in LPL-deficient neurons. These results verified the properties of synaptic activity in LPL-deficient neurons and provide fundamental information to further explore the role of LPL in synaptic function and its underlying mechanism.

EXPERIMENTAL PROCEDURES

Animals

LPL-deficient mice and littermate control C57BL/6J mice were bred in the animal facility of the Peking University Health Science Center. The mice handlings in this study were approved by the Peking University Institutional Animal Care and Use Committee. Genotyping was performed by polymerase chain reaction (PCR). Adult mice were housed under standard conditions in conventional cages and kept on standard chow diet and water *ad libitum* with 12-h light and dark cycles (Xian et al., 2009). A total of 148 mice (including fetus) were used in this study.

Hippocampal slices preparation

The electrophysiology study was performed according to our previous description (Chen et al., 2008). Coronal hippocampal slices with a thickness of 350 μm from postnatal day 10 to 12 male mice were prepared in ice-cold low-Ca^{2+} slicing solution containing (in mM): 119 NaCl, 2.5 KCl, 10 glucose, 1 NaH_2PO_4, 26 $NaHCO_3$, 5 $MgCl_2$, and 0.1 $CaCl_2$ (pH 7.4, with 95% O_2 and 5% CO_2). The hippocampal slices were incubated for 1 h at room temperature (20–24 °C) in standard oxygenated external solution containing (in mM): 119 NaCl, 2.5 KCl, 10 glucose, 1 NaH_2PO_4, 26 $NaHCO_3$, 1.3 $MgCl_2$, and 2 $CaCl_2$ (pH 7.4, with 95% O_2 and 5% CO_2).

Patch clamp recording in hippocampal slices

Whole-cell recordings were performed in hippocampal CA1 pyramidal neurons using an EPC-9/2 amplifier and Pulse software (HEKA Elektronik, Lambrecht/Pfalz, Germany) as described previously (Chen et al., 2008). Membrane potential was voltage-clamped at −70 mV. Signals were filtered at 2 kHz. Patch electrodes were fabricated from glass capillary tubes with filaments and coated with dental wax. Resistance of these pipettes was 4–6 MΩ. Series resistance was < 20 MΩ and compensated to 70–90%. The intercellular solution contained (in mM): 146.5 K-gluconate, 7.5 KCl, 9 NaCl, 1 $MgCl_2$, 10 HEPES, 0.2 EGTA, and 2 ATP-Na_2 (pH 7.2, 300 mOsm).

For miniature excitatory postsynaptic currents (mEPSCs), 1 μM Tetrodotoxin (TTX, Sigma St. Louis, MO, USA) and 10 μM bicuculline (Sigma, St. Louis, MO, USA) were added to the recording bath. Each mEPSC event was fully characterized by amplitude, frequency, half-width and charges. These parameters were detected and analyzed by MiniAnalysis software (Synaptosoft, Inc., Leonia, NJ, USA). The following detection parameters were used: Threshold (pA): eight; Period to search a local maximum (ms): 50; Time before a peak for baseline (ms): 10; Period to search a decay time (ms): 60; Fraction of peak to find a decay time: 0.37; Period to average a baseline (ms): 20; Area threshold: 80; Number of points to average for peak: three. After the software selected individual events, each detected event was visually inspected to eliminate artifacts.

Excitatory postsynaptic currents (EPSCs) were elicited by electrical stimulation of Schaffer collaterals with a bipolar electrode placed in the stratum radiatum, or roughly 150 μm from the recorded CA1 pyramidal neuron. A single pulse (10–150 μA for 0.2 ms) was generated by a Grass stimulator (S88; Grass Instruments, Warwick, RI, USA) and delivered through an isolation unit. EPSCs were recorded at −70 mV in the presence of 10 μM bicuculline. To calculate the AMPA/N-methyl-D-aspartic acid (NMDA) ratio, the amplitudes of AMPA (a-amino-3-hydroxy-5-methyl-4-isoxa-zolep-propionate) current were determined by subtracting the baseline current (obtained by averaging the period 3 ms before the stimulus) from the peak current of the EPSC with holding potential at −70 mV, while the amplitude of NMDA current was measured 50 ms after the peak of the current with holding potential at +40 mV (Myme et al., 2003).

Readily releasable pool (RRP) was depleted with a train of 40 action potentials (AP) at 20 Hz or 500-mOsm sucrose. RRP size was calculated with cumulative amplitude and cumulative charge transfer separately (Schneggenburger et al., 1999; Stevens and Williams, 2007). For the rescue experiment, physiological concentration of DHA (2.7 mg/ml) and AA (2.7 mg/ml) in dimethyl sulfoxide (DMSO) was added to the condition medium of primary hippocampal neurons from LPL-deficient mice 48 h before the experiment while C18:0 fatty acid (2.7 mg/ml) in DMSO was added as control reagent. Same amount of DMSO was added to wild-type (WT) and LPL (no supplement) group. For paired-pulse facilitation, two stimuli were applied at an interval of 20–100 ms, and 6–10 sweeps were averaged to obtain one paired-pulse EPSC trace. The amplitude of the first EPSC was < 50% of maximal evoked EPSC by adjusting the intensity of pulse stimuli. Paired-pulse ratio was defined as $EPSC_2/EPSC_1$ (Mennerick and Zorumski, 1995). The field excitatory postsynaptic potentials (fEPSPs) were recorded in the stratum radiatum of area CA1 with electrodes filled with standard external solution (resistance, 2–4 MΩ). Baseline fEPSPs were monitored by delivering stimuli at 0.1 Hz. fEPSPs were acquired and measured using pClamp 10 (Molecular Devices, Foster City, CA, USA). Post-tetanic potentiation (PTP) was induced by a single burst of 100 pulses at 100 Hz. These parameters were detected and analyzed by Igor pro 4.0 (WaveMetrics, Inc., Lake Oswego, OR, USA).

Lipid extraction and analysis

Hippocampal tissue was processed by a one-step homogenization/extraction/methylation method according to Garces and Mancha (1993). About 0.1 g of sample was weighed and placed into a Pyrex tube. 2 ml of heptane, 1.4 ml of freshly made aqueous reagent (methanol: 2, 2-dimethyl-3-pentanol: H_2SO_4 = 85:11:4 by volume) and 1.6 ml of organic reagent (heptanes: toluene = 63:37

by volume) were added. Freshly prepared di-heptadecanoyl-phosphatidylcholine (Matreya, Inc., Pleasant Gap, PA, USA) was also added as an internal standard before extraction. After mixing the contents, the tubes were placed in a shaking water bath at 80 °C for 2 h. Upon cooling, tubes were thoroughly vortexed to yield a homogeneous solution similar in appearance to tissue homogenized by a rotary blade homogenizer. 2 ml of saturated NaCl was added, and after vortexing, phase separation was accomplished by centrifugation at 3500 rpm for 10 min. The organic layer was removed by nitrogen evaporation. All purified fatty acid methyl esters (FAME) were dissolved in 200 μl heptane and stored in a −20 °C freezer until analysis.

Total FAME was analyzed by Gas Chromatography–Mass Spectrometry (GC–MS, Agilent 6890N-5975 inert MSD). Each fatty acid was identified by GC-Covalent Adduct Chemical Ionization tandem mass spectrometry (Michaud et al., 2002). Quantitative profiles were calibrated using methyl-17:0 as an internal standard and an equal weight FAME mixture (68A; Nu-chek-Prep, Elysian, MN, USA) to derive response factors for each FAME. Chromatography conditions and calibration details have been reported previously (Su et al., 1999). The concentration of each fatty acid from 14 to 24 carbons is expressed as μg fatty acid per mg wet tissue weight.

Statistical analysis

Statistics were calculated using functions provided in GraphPad Prism 5 for Windows (GraphPad Software Inc., La Jolla, CA, USA). All data was expressed as mean ± standard error (SEM) and analyzed using unpaired *t*-test and corrected with the Welch's method if variances were not equal. The significance value was set at $p < 0.05$.

RESULTS

Reduced frequency of mEPSCs in LPL-deficient neurons

To investigate the basic synaptic function of LPL-deficient mice, we first examined the properties of mEPSCs in hippocampal CA1 pyramidal neurons from LPL-deficient and WT mice (Fig. 1A). mEPSCs occur spontaneously and normally correspond to single-vesicle fusion events. The frequency of mEPSCs, an indicator of release probability from presynaptic terminal, was significantly decreased in LPL-deficient neurons (WT, 0.80 ± 0.08 Hz, $n = 12$ neurons; LPL-d, 0.18 ± 0.02 Hz, $n = 15$ neurons, $p < 0.001$) (Fig. 1D). Cumulative frequency distribution of inter-event intervals revealed rightward shifts in LPL-deficient neurons (Fig. 1E), consistent with a comparable reduction in mEPSCs frequency. In contrast, there was no significant difference in amplitude of mEPSCs between WT and LPL-deficient neurons (WT, 21.40 ± 0.98 pA, $n = 12$ neurons; LPL-d, 19.07 ± 0.87 pA, $n = 15$ neurons, $p = 0.09$), which indicates that the responsiveness and number of postsynaptic receptors were not affected in LPL-deficient neurons (Fig. 1F, G). Moreover, of the mEPSCs analysis showed

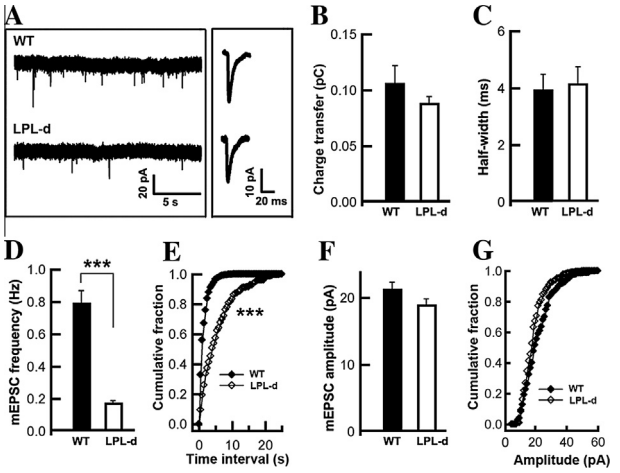

Fig. 1. Reduced frequency of miniature excitatory postsynaptic currents in LPL-deficient neurons. (A) Reprehensive traces of mEPSCs in hippocampal CA1 pyramidal neurons recorded from WT (upper left), and LPL-deficient mice (lower left) in the presence of bicuculline (10 μM) and Tetrodotoxin (TTX, 1 μM), and averaged mEPSC events from WT (upper right) and LPL-deficient neurons (lower right). (B, C) Bar graphs of charge transfer (B: WT, 0.11 ± 0.02 pC, $n = 12$ neurons; LPL-d, 0.09 ± 0.01 pC, $n = 15$ neurons, $p = 0.42$) and half-width (C: WT, 3.97 ± 0.55 ms, $n = 12$ neurons; LPL-d, 4.19 ± 0.61 ms, $n = 15$ neurons, $p = 0.74$) for WT and LPL-deficient neurons. LPL deficiency has no significant influence on vesicle content or single-vesicle fusion kinetics. (D) Bar graphs of mEPSCs frequency in WT and LPL-deficient neurons. LPL-deficient neurons exhibit significantly lower mEPSCs frequency compared to WT neurons (WT, 0.80 ± 0.08 Hz, $n = 12$ neurons; LPL-d, 0.18 ± 0.02 Hz, $n = 15$ neurons, $p < 0.001$). (E) Cumulative distributions of inter-event intervals. Inter-event intervals in LPL-deficient neurons were longer than those of WT neurons ($p < 0.001$, Kolmogorov–Smirnov test). Only event intervals < 20 s were plotted, and three data points from LPL-deficient neurons with intervals of 52, 60, and 61 s were omitted in this plot. F, G, Averaged mEPSC amplitudes (F: WT, 21.40 ± 0.98 pA, $n = 12$ neurons; LPL-d, 19.07 ± 0.87 pA, $n = 15$ neurons, $p = 0.09$) and cumulative distribution of mEPSC amplitudes (G) from WT and LPL-deficient neurons were comparable. LPL-d (LPL deficiency).

no significant difference in half-width (WT, 3.97 ± 0.55 ms, $n = 12$ neurons; LPL-d, 4.19 ± 0.61 ms, $n = 15$ neurons, $p = 0.74$) and charge transfer (WT, 0.11 ± 0.02 pC, $n = 12$ neurons; LPL-d, 0.09 ± 0.01 pC, $n = 15$ neurons, $p = 0.42$) between WT and LPL-deficient neurons (Fig. 1B, C). Thus, in LPL-deficient neurons, the propensity of vesicles released from the presynaptic terminal decreased without significantly altering the neurotransmitter content of vesicles or the kinetics of single-vesicle fusion (Bekkers et al., 1990).

LPL-deficient neurons presented normal evoked excitatory postsynaptic currents with single-pulse stimulation

To further investigate the properties of synaptic transmission in LPL-deficient neurons, we examined evoked EPSCs. Electric stimuli (0.1 Hz) were applied to CA3 Schaffer collateral using bipolar electrodes, and EPSCs of hippocampal CA1 pyramidal neurons were recorded by whole-cell patch clamp at −70 mV in brain slices. The mean amplitude (WT, 167.07 ± 20.06 pA, $n = 11$ neurons; LPL-d, 145.01 ± 20.95 pA, $n = 10$

neurons; $p = 0.47$), charge transfer (WT, 8.18 ± 1.43 pC, $n = 11$ neurons; LPL-d, 7.22 ± 1.28 pC, $n = 10$ neurons; $p = 0.63$), and half-width of EPSCs (WT, 17.20 ± 2.63 ms, $n = 11$ neurons; LPL-d, 16.29 ms ± 0.91, $n = 10$ neurons; $p = 0.72$) from LPL-deficient neurons were not significantly different from WT neurons (Fig. 2A). Consistently, input/output curve showed no significant change in synaptic strength (Fig. 2B, $p > 0.05$). These results suggest that the properties of neurotransmitter release in response to single AP do not markedly change in hippocampal synapses of LPL-deficient neurons.

In particular, with 2 mM Mg^{2+} in the recording bath, EPSCs recorded under voltage clamping at −70 mV were primarily mediated by AMPA receptors. Similar to AMPA receptor-mediated EPSCs, the NMDA receptor-mediated EPSCs recorded at +40 mV holding potential did not significantly differ between LPL-deficient neurons and control neurons (data not shown). Consequently, the AMPA/NMDA ratio, which reflects postsynaptic receptors distribution, showed no significant difference between LPL-deficient and WT neurons (WT, 2.28 ± 0.21, $n = 6$ neurons; LPL-d, 2.41 ± 0.16, $n = 6$ neurons, $p = 0.36$, Fig. 2C). In addition, we previously reported that levels of postsynaptic density protein 95 (PSD-95) were not significantly different in LPL-deficient mice (Xian et al., 2009). These results suggest no significant impairment of postsynaptic receptors in LPL-deficient neurons.

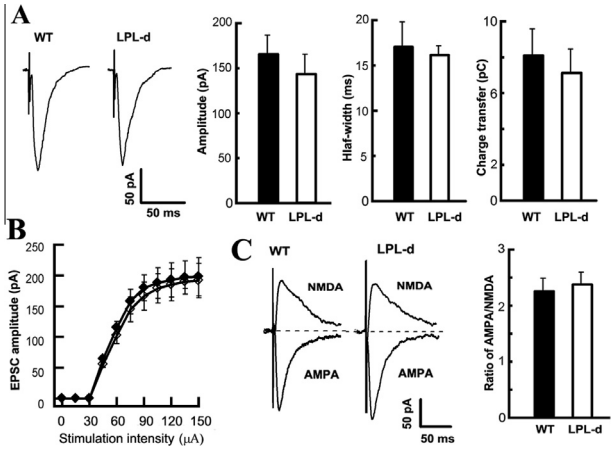

Fig. 2. LPL-deficient neurons presented normal evoked excitatory postsynaptic currents with single-pulse stimulation. (A) Representative traces of evoked EPSCs by whole-cell recordings recorded from WT and LPL-deficient neurons (left panel). Relative to their WT controls ($n = 11$ neurons), LPL-deficient neurons ($n = 10$ neurons) exhibited no significant difference in the amplitude (WT, 167.07 ± 20.06 pA; LPL-d, 145.01 ± 20.95 pA, $p = 0.47$), half-width (WT, 17.20 ± 2.63 ms; LPL-d, 16.29 ms ± 0.91, $p = 0.72$) or charge transfer (WT, 8.18 ± 1.43 pC; LPL-d, 7.22 ± 1.28 pC, $p = 0.63$) of EPSCs. (B) The basal synaptic transmission from LPL-deficient and WT mice was identical, as shown by plotting varying stimulus intensity against EPSC amplitude ($p > 0.05$). (C) Representative traces of evoked EPSCs mediated by AMPA receptors and NMDA receptors separately recorded from WT and LPL-deficient neurons (left panel). AMPA current was measured at the peak of current at −70 mV, while the NMDA current was measured at 50 ms after the peak of the current at +40 mV. Bar graphs of AMPA/NMDA ratio for WT and LPL-deficient neurons (right panel). No significant difference was observed (WT, 2.28 ± 0.21, $n = 6$ neurons; LPL-d, 2.41 ± 0.16, $n = 6$ neurons, $p = 0.36$).

Presynaptic dysfunction in LPL-deficient neurons

Since RRP is generally considered to be the fusion-competent population of vesicles and is related to presynaptic release probability (Rosenmund and Stevens, 1996; Dobrunz, 2002), we wondered whether the reduced frequency of mEPSCs (Fig. 1D, E) resulted from the alteration of RRP size in LPL-deficient neurons. Applying a train of stimuli (40 AP at 20 Hz) to deplete the RRP in CA1 neurons (Fig. 3Aa), we found that total charge transfer, which represents the RRP size, was significantly smaller in LPL-deficient neurons than WT neurons (WT, 4.41 ± 0.17 nC, $n = 8$; LPL-d, 3.63 ± 0.16 nC; $n = 8$, $p < 0.01$, Fig. 3Ab). Cumulative amplitude analysis (Schneggenburger et al., 1999; Stevens and Williams, 2007) also confirmed a smaller RRP size in LPL-deficient neurons (WT, 0.64 ± 0.01 nA, $n = 7$; LPL-d, 0.37 ± 0.03 nA, $n = 6$, $p < 0.001$, Fig. 3Ac, Ad), which supports our observation of significantly reduced docking vesicles and decreased frequency of mEPSCs (Fig. 1D, E).

To investigate whether reduced RRP size impairs the presynaptic function in LPL-deficient neurons, we further analyzed the paired-pulse behavior of the EPSCs with stimulations spaced at intervals of 10–100 ms. The ratio of $EPSC_2/EPSC_1$, an indicator of presynaptic function,

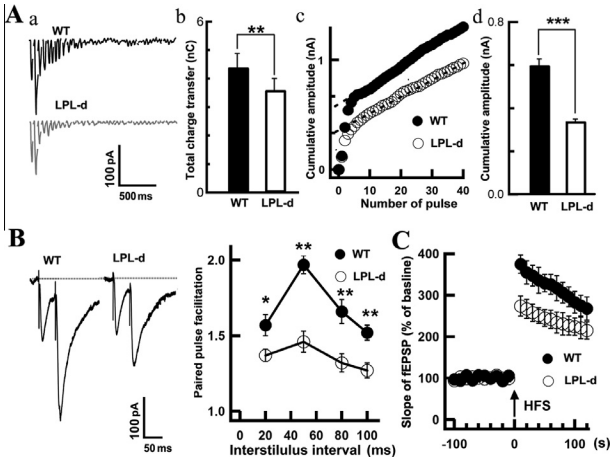

Fig. 3. Presynaptic dysfunction in LPL-deficient neurons. (A) Representative traces in response to RRP depletion train 40 AP, 20 Hz (a). Normalized RRP measured with total charge transfer (b: WT, 4.41 ± 0.17 nC, $n = 8$ neurons; LPL-d, 3.63 ± 0.16 nC; $n = 8$ neurons, $p < 0.01$,) and cumulative amplitude (c, d: WT, 0.64 ± 0.01 nA, $n = 7$ neurons; LPL-d, 0.37 ± 0.03 nA, $n = 6$ neurons, $p < 0.001$) was significantly decreased in LPL-deficient neurons. (B) Representative traces with a 50-ms interval recorded from WT and LPL-deficient neurons in response to paired stimulus (left panel). Paired-pulse ratio, defined as the ratio of evoked EPSC amplitudes (EPSC2/EPSC1), was significantly different between WT and LPL-deficient neurons at different ISI (ISI 50 ms: WT, 1.97 ± 0.06, $n = 7$ neurons; LPL-d, 1.46 ± 0.08, $n = 9$ neurons, $p < 0.01$, right panel). (C) PTP impairment in the hippocampal slices of LPL-deficient mice compared to that of WT mice (WT, 268 ± 17.7%, $n = 5$ neurons; LPL-deficient 215.1 ± 20.6%, $n = 5$ neurons, $p < 0.05$). The fEPSP was given as percentage of the baseline slope. The arrow indicates titanic stimulation.

significantly decreased for different inter-stimuli intervals (ISI) in LPL-deficient neurons (ISI 50 ms: WT, 1.97 ± 0.06, n = 7 neurons; LPL-d, 1.46 ± 0.08, n = 9 neurons, p < 0.01, Fig. 3B).

We then tested the PTP, which exclusively reflects presynaptic plasticity. PTP was induced by one train of HFS (100 Hz, 1 s) in the CA1 region from LPL-deficient mice (n = 5 neurons) or their WT controls (n = 5 neurons). By 120 s, the slope of fEPSPs from WT mice were potentiated to 268 ± 17.7% of baseline, whereas the slope of fEPSPs from LPL-deficient mice decayed to 215.1 ± 20.6% of baseline (p < 0.05, Fig. 3C). These results indicate reduced RRP size in LPL-deficient neurons ultimately impaired presynaptic function and plasticity.

Impaired synaptic vesicle recycling in LPL-deficient neurons

RRP recycling is crucial for maintaining RRP size in active synapses (Sudhof, 2004). In order to test whether reduced RRP size in LPL-deficient neurons resulted from impaired synaptic vesicle recycling, we applied two trains of stimuli (40 AP at 20 Hz for each train) with different time intervals. The first train led to a depletion of the RRP and the second train determined the extent of RRP recycling during the inter-stimulus interval, thereby allowing refill properties to be studied (Stevens and Williams, 2007). We found a slower RRP recovery in LPL-deficient neurons at intervals of 5 s (WT, 72.24 ± 6.58%, n = 5 neurons; LPL-d, 54.93 ± 5.21%, n = 5 neurons, p < 0.01, Fig. 4A), 10 s (WT, 83.87 ± 5.54%, n = 5 neurons; LPL-d, 61.56 ± 4.55%, n = 5 neurons, p < 0.01, Fig. 4A) and 20 s (WT, 88.44 ± 5.49%, n = 5 neurons; LPL-d, 73.03 ± 5.94%, n = 5 neurons, p < 0.05, Fig. 4A).

DHA and AA partially rescue synaptic vesicle recycling of LPL-deficient neurons

Previous studies found that PUFA contents, which could enhance synaptic vesicle recycling, decreased in the hippocampus of LPL-deficient mice (Wang et al., 2011). Using lipid assay, we found DHA (WT, 14.06 ± 0.23%, n = 9; LPL-d, 13.06 ± 0.16%, n = 9; p < 0.01; Fig. 4B, left panel) and AA (WT, 11.66 ± 0.23%, n = 9; LPL-d, 10.83 ± 0.19%, n = 9; p < 0.05; Fig. 4B, left panel) decreased in the hippocampus of LPL-deficient mice compared to WT mice without a significant difference in total lipids (WT, 13.54 ± 0.09 μg/mg, n = 9; LPL-d, 13.26 ± 0.11 μg/mg, n = 9; p = 0.09, Fig. 4B, right panel). To further understand the roles of DHA and AA in synaptic vesicle recycling in LPL-deficient neurons, we exogenously applied DHA and AA to the conditional medium of primary cultured hippocampal neurons. 500-mOsm sucrose was applied with different stimulus intervals to test the function of DHA or AA in RRP recycling, significant difference was observed between WT and LPL-deficient neurons (For 5 s ISI: WT, 63.37 ± 7.4%, n = 10, LPL = 39.21 ± 6.8%, n = 10, p < 0.01, Fig. 4C). Exogenously DHA or AA supplement could partially restore the defect (For 5 s ISI: LPL + AA, 52.4 ± 6.3%, n = 10, p < 0.01; LPL + DHA = 53.6 ± 5.7%, n = 10, p < 0.01, Fig. 4C) while C18:0 showed no effect (LPL + C18:0, 35.9 ± 4.6%, n = 8, p = 0.21, Fig. 4C).

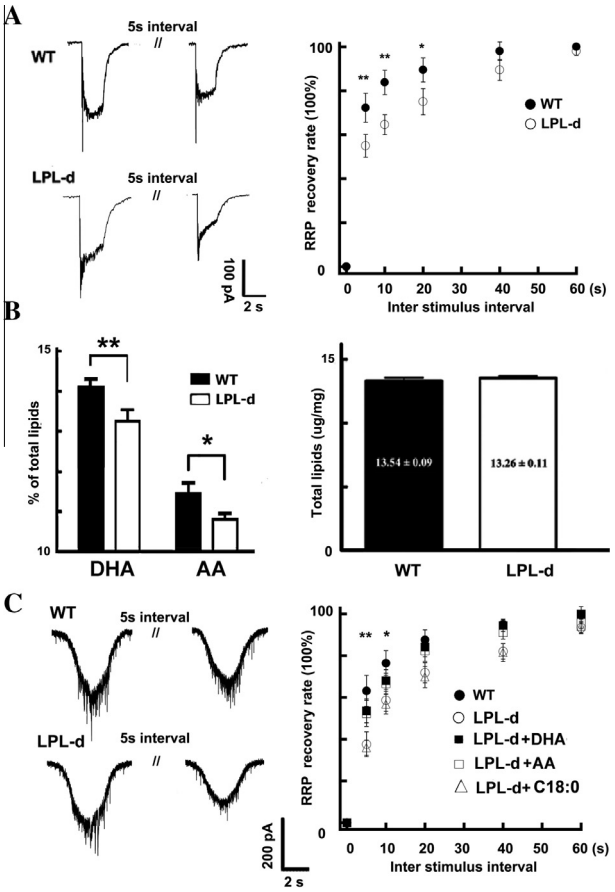

Fig. 4. Impaired synaptic vesicle recycling in LPL-deficient neurons. (A) Representative traces recorded from WT and LPL-deficient neurons in response to double trains of stimuli (20 Hz, 40 AP) (left panel). Defining RRP_{2nd}/RRP_{1st} as RRP recovery rate, LPL-deficient neurons exhibited different kinetics of RRP recovery rate compared to their WT controls at different inter-stimulus intervals (For a 5-s interval: WT, 72.24 ± 6.58%, n = 5 neurons; LPL-d, 54.93 ± 5.21%, n = 5 neurons, p < 0.01, right panel). (B) Docosahexaenoic acid (DHA) or arachidonic acid (AA) in the hippocampus was decreased in LPL-deficient mice (n = 9) compared to WT controls (n = 9, left panel). (C) Representative traces recorded from WT and LPL-deficient neurons in response to 500-mOsm sucrose RRP deletion stimuli (left panel). LPL-deficient neurons exhibited slower RRP recovery compared to WT neurons at different inter-stimulus intervals (For 5 s ISI: WT, 63.37 ± 7.4%, n = 10 neurons; LPL, 39.21 ± 6.8%, n = 10 neurons, p < 0.01). Exogenously DHA or AA supplement could partially restore the defect (For 5 s ISI: LPL + AA, 52.4 ± 6.3%, n = 10 neurons, p < 0.01; LPL + DHA = 53.6 ± 5.7%, n = 10 neurons, p < 0.01) while C18:0 showed no effect (LPL + C18:0, 35.9 ± 4.6%, n = 8 neurons, p = 0.27; right panel).

DISCUSSION

LPL was identified in the brain with high expression in the hippocampus (Goldberg et al., 1989; Yacoub et al., 1990) and localized in soma and presynaptic vesicles (Klinger et al., 2011). Epidemiological investigations revealed that some mutant LPL genes were associated with dementia symptoms as well as hippocampal dysfunction. However, the effects of LPL on synaptic function are still unclear.

Our previous paper reported no change in hippocampus structure, synapse number and PSD-95 while synaptic vesicles and presynaptic synaptophysin levels were significantly decreased in LPL-deficient mice (Xian et al., 2009). In this study, analysis of mEPSCs in LPL-deficient neurons primarily showed fewer presynaptic release events without differences in fusion process, neurotransmitter content or postsynaptic receptors. Input–output curve and AMPA/NMDA ratio of evoked EPSCs confirmed normal functional postsynaptic receptors, while reduced PPF and RRP size in LPL-deficient neurons indicate presynaptic dysfunction. Therefore, we hypothesize that basic synaptic transmission was not affected but synaptic activity-dependent release was reduced and ultimately resulted in presynaptic dysfunction and plasticity impairment due to LPL deficiency.

To maintain synaptic transmission during intense neuronal activity, RRP is effectively replenished by recruitment of synaptic vesicles. In our study, impairment of synaptic vesicle recycling was identified with electrophysiological experiments and FM imaging experiments. Compared to our previous report, the reduction in RRP is smaller. Besides error caused by different methods, the movement of vesicles in active synapse may partially compensate for the defect in presynaptic vesicles and impaired synaptic endocytosis. Otherwise, synaptic vesicle recycling may not be the only factor leading to reduced synaptic vesicles.

PUFAs play an important role in synaptic function (Lafourcade et al., 2011). Previous studies have reported omega-3 PUFAs to promote clathrin-mediated endocytosis (CME) and synaptic vesicle recycling (Marza et al., 2008; Ben Gedalya et al., 2009). Synaptic vesicle recycling is the major, if not exclusive, mechanism to maintain RRP size in active hippocampal synapse. In this study, we found DHA and AA – the major components of PUFAs – decreased in the hippocampus of LPL-deficient mice. PUFA metabolism seems to be affected by neuronal LPL deficiency (Wang et al., 2011), but it is not clear how LPL regulates PUFA content in the brain. Based on previous studies, LPL deficiency may lead to inhibition of PUFA release from lipoproteins and thus insufficient PUFA supply for neurons. In our rescue experiment, no significant difference was observed in acute test with DHA and AA treatment less than 12 h, which indicates that metabolism is necessary to rescue synaptic vesicle recycling. A hypothetical biological target for PUFA activation is certain classes of membrane phospholipids and specifically phosphoinositides that are known to regulate CME, but we cannot exclude the direct effect of DHA and AA as free fatty acids. Previous research found that membrane PUFAs act as cone-shaped lipids that produce a positive curvature of the membrane leaflet, inducing invagination and fission of the membrane and thereby enhancing membrane trafficking. Moreover, PUFA can alter actual protein levels of specific key factors in CME, such as clathrin. Therefore, PUFAs may affect synaptic vesicle recycling in multiple ways.

As an enzyme, LPL regulates the metabolism of many lipids. Other than DHA and AA, several lipids are involved in synaptic endocytosis and synaptic vesicle recycling. We did not observe significant alteration in PIP2 and cholesterol, which are known for their role in synaptic endocytosis and synaptic vesicle recycling (Cremona et al., 1999; Pechstein et al., 2010). However, we cannot exclude the potential involvement of other related lipids that could explain failure for DHA or AA supplements to completely rescue synaptic vesicle recycling impairment. Lipids or lipid-related factors could also influence presynaptic dysfunction in LPL-deficient mice in other ways. We previously found a significant reduction of vitamin E in the hippocampus of LPL-deficient mice (Xian et al., 2009). Vitamin E supplement could improve the health of culture neurons after DIV 20 but show no effect on synaptic vesicle recycling (data not shown). Therefore, Vitamin E might provide neuron protection through another mechanism. These studies indicate a potential role of LPL in synaptic function and provide important information to further explore the function and mechanism of LPL in learning and memory.

CONFLICT OF INTEREST

There are no actual or potential conflicts of interest.

Acknowledgments—This work was supported by the National High Technology Research and Development Program of China (973 Program No. 2012CB911000, 2012CB911004), the National Natural Science Foundation of China (NSFC; Grants Nos. 81171015 and 81371205) and NSFC-JSPS (Grant No. 81211140047). We thank Dr. Michael Hayden (University of British Columbia, Centre for Molecular Medicine and Therapeutics, Vancouver, Canada) for supplying LPL-deficient mice.

REFERENCES

Baum L, Chen L, Masliah E, Chan YS, Ng HK, Pang CP (1999) Lipoprotein lipase mutations and Alzheimer's disease. Am J Med Genet 88:136–139.

Bekkers JM, Richerson GB, Stevens CF (1990) Origin of variability in quantal size in cultured hippocampal neurons and hippocampal slices. Proc Natl Acad Sci USA 87:5359–5362.

Ben Gedalya T, Loeb V, Israeli E, Altschuler Y, Selkoe DJ, Sharon R (2009) Alpha-synuclein and polyunsaturated fatty acids promote clathrin-mediated endocytosis and synaptic vesicle recycling. Traffic 10:218–234.

Ben-Zeev O, Doolittle MH, Singh N, Chang CH, Schotz MC (1990) Synthesis and regulation of lipoprotein lipase in the hippocampus. J Lipid Res 31:1307–1313.

Chait A, Robertson HT, Brunzell JD (1981) Chylomicronemia syndrome in diabetes mellitus. Diabetes Care 4:343–348.

Chen XW, Feng YQ, Hao CJ, Guo XL, He X, Zhou ZY, Guo N, Huang HP, Xiong W, Zheng H, Zuo PL, Zhang CX, Li W, Zhou Z (2008) DTNBP1, a schizophrenia susceptibility gene, affects kinetics of transmitter release. J Cell Biol 181:791–801.

Cremona O, Di Paolo G, Wenk MR, Luthi A, Kim WT, Takei K, Daniell L, Nemoto Y, Shears SB, Flavell RA, McCormick DA, De Camilli P (1999) Essential role of phosphoinositide metabolism in synaptic vesicle recycling. Cell 99:179–188.

Dobrunz LE (2002) Release probability is regulated by the size of the readily releasable vesicle pool at excitatory synapses in hippocampus. Int J Dev Neurosci 20:225–236.

Garces R, Mancha M (1993) One-step lipid extraction and fatty acid methyl esters preparation from fresh plant tissues. Anal Biochem 211:139–143.

Goldberg IJ, Soprano DR, Wyatt ML, Vanni TM, Kirchgessner TG, Schotz MC (1989) Localization of lipoprotein lipase mRNA in selected rat tissues. J Lipid Res 30:1569–1577.

Heilman KM, Fisher WR (1974) Hyperlipidemic dementia. Arch Neurol 31:67–68.
Klinger SC, Glerup S, Raarup MK, Mari MC, Nyegaard M, Koster G, Prabakaran T, Nilsson SK, Kjaergaard MM, Bakke O, Nykjaer A, Olivecrona G, Petersen CM, Nielsen MS (2011) SorLA regulates the activity of lipoprotein lipase by intracellular trafficking. J Cell Sci 124:1095–1105.
Lafourcade M, Elezgarai I, Mato S, Bakiri Y, Grandes P, Manzoni OJ (2007) Molecular components and functions of the endocannabinoid system in mouse prefrontal cortex. PLoS One 2:e709.
Lafourcade M, Larrieu T, Mato S, Duffaud A, Sepers M, Matias I, De Smedt-Peyrusse V, Labrousse VF, Bretillon L, Matute C, Rodriguez-Puertas R, Laye S, Manzoni OJ (2011) Nutritional omega-3 deficiency abolishes endocannabinoid-mediated neuronal functions. Nat Neurosci 14:345–350.
Marza E, Long T, Saiardi A, Sumakovic M, Eimer S, Hall DH, Lesa GM (2008) Polyunsaturated fatty acids influence synaptojanin localization to regulate synaptic vesicle recycling. Mol Biol Cell 19:833–842.
Mead JR, Irvine SA, Ramji DP (2002) Lipoprotein lipase: structure, function, regulation, and role in disease. J Mol Med 80:753–769.
Mennerick S, Zorumski CF (1995) Paired-pulse modulation of fast excitatory synaptic currents in microcultures of rat hippocampal neurons. J Physiol 488(Pt 1):85–101.
Merkel M, Eckel RH, Goldberg IJ (2002) Lipoprotein lipase: genetics, lipid uptake, and regulation. J Lipid Res 43:1997–2006.
Michaud AL, Diau GY, Abril R, Brenna JT (2002) Double bond localization in minor homoallylic fatty acid methyl esters using acetonitrile chemical ionization tandem mass spectrometry. Anal Biochem 307:348–360.
Myme CI, Sugino K, Turrigiano GG, Nelson SB (2003) The NMDA-to-AMPA ratio at synapses onto layer 2/3 pyramidal neurons is conserved across prefrontal and visual cortices. J Neurophysiol 90:771–779.
Pechstein A, Bacetic J, Vahedi-Faridi A, Gromova K, Sundborger A, Tomlin N, Krainer G, Vorontsova O, Schafer JG, Owe SG, Cousin MA, Saenger W, Shupliakov O, Haucke V (2010) Regulation of synaptic vesicle recycling by complex formation between intersectin 1 and the clathrin adaptor complex AP2. Proc Natl Acad Sci USA 107:4206–4211.
Rohrbough J, Broadie K (2005) Lipid regulation of the synaptic vesicle cycle. Nat Rev Neurosci 6:139–150.
Rosenmund C, Stevens CF (1996) Definition of the readily releasable pool of vesicles at hippocampal synapses. Neuron 16:1197–1207.
Schneggenburger R, Meyer AC, Neher E (1999) Released fraction and total size of a pool of immediately available transmitter quanta at a calyx synapse. Neuron 23:399–409.
Stevens CF, Williams JH (2007) Discharge of the readily releasable pool with action potentials at hippocampal synapses. J Neurophysiol 98:3221–3229.
Su HM, Bernardo L, Mirmiran M, Ma XH, Corso TN, Nathanielsz PW, Brenna JT (1999) Bioequivalence of dietary alpha-linolenic and docosahexaenoic acids as sources of docosahexaenoate accretion in brain and associated organs of neonatal baboons. Pediatr Res 45:87–93.
Sudhof TC (2004) The synaptic vesicle cycle. Annu Rev Neurosci 27:509–547.
Vilaro S, Camps L, Reina M, Perez-Clausell J, Llobera M, Olivecrona T (1990) Localization of lipoprotein lipase to discrete areas of the guinea pig brain. Brain research 506:249–253.
Wang H, Astarita G, Taussig MD, Bharadwaj KG, DiPatrizio NV, Nave KA, Piomelli D, Goldberg IJ, Eckel RH (2011) Deficiency of lipoprotein lipase in neurons modifies the regulation of energy balance and leads to obesity. Cell Metab 13:105–113.
Xian X, Liu T, Yu J, Wang Y, Miao Y, Zhang J, Yu Y, Ross C, Karasinska JM, Hayden MR, Liu G, Chui D (2009) Presynaptic defects underlying impaired learning and memory function in lipoprotein lipase-deficient mice. J Neurosci 29:4681–4685.
Yacoub LK, Vanni TM, Goldberg IJ (1990) Lipoprotein lipase mRNA in neonatal and adult mouse tissues: comparison of normal and combined lipase deficiency (cld) mice assessed by in situ hybridization. J Lipid Res 31:1845–1852.

(Accepted 21 July 2014)
(Available online 3 September 2014)